

Research Paper

Multi-objective optimization of energy-efficient retrofitting strategies for single-family residential homes: Minimizing energy consumption, CO₂ emissions and retrofit costs

Džana Kadrić^a, Amar Aganović^{b,*}, Edin Kadrić^a

^a Faculty of Mechanical Engineering, University of Sarajevo, Bosnia and Herzegovina

^b Department of Automation and Process Engineering, The Arctic University of Tromsø, Norway

ARTICLE INFO

Article history:

Received 30 May 2023

Received in revised form 13 August 2023

Accepted 29 August 2023

Available online xxxx

Keywords:

Building retrofit

Multi-objective optimization

Energy efficiency

Retrofit costs

CO₂ emissions

Pareto-optimal solutions

ABSTRACT

The retrofitting of buildings for improved energy efficiency has been recognized as crucial for achieving climate mitigation goals in Bosnia and Herzegovina (B&H). However, performing multi-objective optimizations for retrofitting existing buildings poses challenges, as it requires balancing conflicting objectives such as retrofit costs, energy savings, and CO₂ reduction. To tackle this challenge, we employed a multi-objective analysis approach that aims to identify Pareto-optimal solutions for retrofitting, striking a balance between energy consumption, CO₂ emissions, and retrofit costs. In this study, we utilized a combination of Full Factorial Design (FFD) and the state-of-the-art NSGA-III framework to evaluate energy-efficient (EE) retrofit strategies for residential buildings in B&H. The analysis was based on the existing building database from the national TABULA study, serving as a fundamental reference. By analyzing this data, we aimed to determine the optimal approach for EE retrofitting in single-family homes (SFH). Key results indicate that upgrading external walls and improving heating system efficiency are the most effective measures for reducing energy consumption and CO₂ emissions. However, these measures come with higher retrofit costs. A multi-objective optimization approach identifies a set of non-dominated solutions representing energy efficiency retrofit measures with the lowest specific final energy for heating, specific CO₂ emissions, and overall retrofit costs. The top-ranked set of measures achieves a Simple Payback Period (SPP) of 19.9 years. The insights gained from this study are intended to provide valuable guidance to decision-makers in formulating cost-effective and energy-efficient retrofitting strategies that simultaneously minimize annual energy consumption, CO₂ emissions, and retrofit costs.

© 2023 The Author(s). Published by Elsevier Ltd. This is an open access article under the CC BY license (<http://creativecommons.org/licenses/by/4.0/>).

1. Introduction

Bosnia and Herzegovina (B&H) is a member state of the Energy Community (EC) and is required to develop policies and implement specific measures in order to achieve greenhouse gas (GHG) emission neutrality by 2050, as defined in various European energy and climate plans (European Parliament and Council of the European Union, 2018; MOFTER, 2021). As B&H aims to align its energy policies with those of the European Union (EU), it is currently in the process of preparing its integrated National Energy and Climate Plan (NECP) for the period 2021–2030 (Energy Community, 2020; Energy Community, 2022). According to NECP, Bosnia and Herzegovina must develop long-term strategic frameworks for the implementation of energy-efficient (EE) retrofit measures in its building stock (Energy Community, 2020; Energy Community,

2022). Given that residential buildings account for 41% of the total energy consumption in the country, with space heating comprising 72% of that total (Official Gazette of Bosnia and Herzegovina, 2017), prioritizing the reduction of energy consumption for domestic space heating in future EE retrofit measures is crucial. Therefore, retrofitting initiatives for buildings are considered to be of strategic importance for achieving national energy-saving targets in both the short and long term (European Commission, 2020; Publications Office of the European Union, 2019). Implementing EE retrofit measures not only reduces the country's GHG emissions and overall energy consumption, but also offers significant economic, environmental, and social benefits (European Commission, 2020; Nydahl et al., 2019; Tuominen et al., 2012; Hashempour et al., 2020). This underscores the current importance of EE measures, which may necessitate the renovation of thousands of buildings each year, including single-family houses, multi-apartment blocks, and high-rise buildings, based on predefined EE measures. To accomplish such an ambitious

* Corresponding author.

E-mail address: amar.aganovic@uit.no (A. Aganović).

objective, it is essential to encourage innovative approaches to enhance the energy efficiency of buildings, focusing on aspects such as the building envelope, energy systems, and the utilization of renewable energy sources (Ruggeri et al., 2020; Pajek et al., 2023).

A comprehensive examination of the cost structure associated with energy-efficient (EE) retrofit measures in the residential sector of B&H is presented in a study conducted by Kadrić et al. (2022b). This study explores the potential of translating EE retrofit measures in the residential sector into a nationwide economic energy-saving policy, aimed at facilitating future subsidies and financial schemes for EE retrofit in B&H. The findings from this study emphasize the urgent need to develop a robust financial subsidy program for homeowners in B&H. Another study, utilizing an optimization model based on the Response Surface Methodology, has identified the building parameters that have the greatest impact on energy savings when implementing EE retrofit measures in B&H (European Commission, 2020). However, the feasibility of large-scale deployment of these retrofit measures may be hindered by economic constraints in low- and middle-income countries (Kadrić et al., 2022b). However, economic constraints in low- and middle-income countries may pose challenges to the large-scale deployment of these retrofit measures (Kadrić et al., 2022b). To address this challenge, a combination of various energy efficiency measures needs to be analyzed to identify the “cost-optimal” package that minimizes overall costs. The evaluation of EE retrofit measures can be based on multiple criteria, including initial investment cost, operational cost, energy consumption, environmental performance, and indoor environmental quality, among others (Kolokotsa et al., 2009; Almeida and Ferreira, 2017; Dolšak, 2023). Achieving robust and effective cost-optimal solutions is therefore a critical task, considering the numerous variables involved in evaluating the performance of building envelopes and energy systems. Consequently, solving optimization problems is typically necessary for the EE retrofitting of buildings, and multi-objective optimization (MOO) techniques have been proven effective in this regard compared to the conventional cost-optimal analysis approach (Ascione et al., 2017). When integrated with building performance simulation tools, MOO techniques enable the consideration of additional EE retrofit objectives beyond minimizing energy consumption (Ascione et al., 2017; Hamdy et al., 2011; Fan and Xia, 2017; Lu et al., 2015; Chantrelle et al., 2011; Mauro et al., 2015; Delgarm et al., 2016b; Baghoolizadeh et al., 2021), such as reducing thermal discomfort (Ascione et al., 2017; Chantrelle et al., 2011), total costs (Lu et al., 2015; Baghoolizadeh et al., 2021), life-cycle environmental impact (Chantrelle et al., 2011), and GHG emissions (Ascione et al., 2017; Hamdy et al., 2011; Fan and Xia, 2017).

The process of selecting the most optimal solutions to support and guide decision-making for energy-efficient (EE) retrofitting can be challenging due to trade-offs among different objectives (Costa-Carrapiço et al., 2020; Evins, 2013; Jafari and Valentin, 2018b,a). In the past, decision-making models for building retrofitting primarily focused on a single criterion prior to 2008 (Hashempour et al., 2020). However, more recent models have incorporated multiple criteria (Chantrelle et al., 2011; Jafari and Valentin, 2018a), in line with the Energy Performance of Buildings Directive (EPBD) Recast (European Parliament and Council of the European Union, 2010), which mandates the selection of energy design and retrofitting approaches based on “cost-optimality” (Ferrara et al., 2019) over a standard calculation period of either 20 years (for non-residential buildings) or 30 years (for residential buildings) (European Parliament and Council of the European Union, 2021). To minimize overall costs, it is necessary to explore and combine several energy efficiency measures

in order to identify the “cost-optimal” package. Therefore, it is crucial to approach these strategies with careful consideration of their cost-effectiveness and technical feasibility.

To address these challenges, numerous studies have adapted multi-objective optimization (MOO) techniques to simultaneously address multiple objectives for EE retrofitting in buildings (Sharif and Hammad, 2019; Yong et al., 2020; Ascione et al., 2019; Zhang et al., 2021; Shen et al., 2019; Roberti et al., 2017; Rosso et al., 2017). For instance, Sharif and Hammad (2019) integrated genetic algorithms (GA) with Pareto solutions to reduce energy consumption, life-cycle cost, and environmental impact in institutional buildings.

Yong et al. (2020) developed a particle swarm optimization tool to simultaneously minimize energy consumption and maximize thermal comfort levels in both office buildings and multi-family homes. Ascione et al. (2019) investigated residential buildings across different Italian climates using a GA-based Pareto optimization approach to minimize primary energy consumption, global cost, and discomfort hours. Zhang et al. (2021) employed non-dominated sorting to identify Pareto-optimal solutions for reducing CO₂ emissions while increasing cost savings in the retrofitting of Canadian residential buildings. Shen et al. (2019) applied the non-dominated sorting differential evolution (NSDE) approach to optimize the retrofit planning of a campus building at the University of Pennsylvania (USA) using Pareto fronts. Roberti et al. (2017) computed NSGA-II-based Pareto-optimal retrofits considering thermal comfort, energy consumption, and conservation compatibility for a medieval building in Northern Italy. Additionally, Rosso et al. (2017) utilized an NSGA-II optimization approach to identify Pareto optimal solutions capable of reducing annual energy demand, energy costs, and CO₂ emissions by more than 40%, while maintaining nearly 60% lower investment costs compared to other criterion-optimal solutions.

Wang (2023) employed a particle swarm algorithm to reduce the cost of energy consumption and improve the predicted mean vote in self-built houses in northern China. Gao et al. (2023) coupled a non-dominated sorting genetic algorithm with Pareto solutions to reduce carbon emissions and energy consumption while ensuring acceptable indoor thermal comfort. Liu and Pouramini (2021) utilized the enhanced water strider optimization algorithm to obtain the Pareto set of optimal solutions for minimizing greenhouse gas emissions and improving thermal comfort in residential buildings.

The findings presented in these studies demonstrate the promising potential of integrating multi-objective optimization (MOO) techniques with Pareto optimal solutions as a decision-making tool for building retrofits in highly developed countries. Among the MOO methods integrated with Pareto optimal solutions, NSGA-II has been the most commonly utilized approach for building retrofit optimization (Delgarm et al., 2016a; Sharif and Hammad, 2017; Mostafazadeh et al., 2023). NSGA-II is renowned for its flexibility and adaptability in solving various optimization problems across different fields, including building retrofit optimization. However, despite its widespread use in making significant advancements in building retrofit, the latest developments in the field, such as NSGA-III, have been overlooked by building performance researchers. NSGA-III, introduced by Deb and Jain (2013) in 2013, is an extension of NSGA-II that addresses its limitations and enhances performance, inheriting all the favorable mechanisms and features of its 12-year-old predecessor. The primary advantage of NSGA-III over NSGA-II lies in its improved ability to handle multiple objectives and achieve an enhanced distribution of solutions (Emmerich and Deutz, 2018; Ishibuchi et al., 2016; Ciro et al., 2016).

In this study, we apply a Full Factorial Design (FFD) integrated NSGA-III framework to assess the energy-efficient (EE)

retrofitting of residential buildings in B&H. Currently, there is a lack of studies utilizing multi-objective optimization techniques for EE retrofitting in low- or middle-income countries like Bosnia and Herzegovina. Our analysis builds upon the existing building database provided by the national TABULA study (Kadrić et al., 2022b) and offers insights into the optimal EE retrofit strategy for single-family homes (SFH). By employing the state-of-the-art NSGA-III algorithm along with FFD, this study not only promotes the use of NSGA-III but also provides valuable insights into the optimal EE retrofit strategy for SFH in a low- or middle-income country—an aspect that has not been previously explored. Decision-makers in countries with similar economic backgrounds can leverage the findings of this study to develop EE retrofit strategies that result in the lowest possible annual energy consumption, CO₂ emissions, and retrofit costs.

The remainder of this paper is organized as follows. Section 2 presents the methodology used, including details about the developed building model, the FFD models employed to establish functional relationships between system responses and various building parameters, as well as the cost structure of energy efficiency (EE) retrofitting. Furthermore, in Section 2, the multi-objective optimization method NSGA-III, utilized to obtain Pareto front solutions, and the composite desirability function used for ranking the Pareto front solutions, are discussed.

Section 3 presents the main results of the study, providing a detailed analysis of the developed models for predicting specific energy for heating, CO₂ emissions, and costs of various EE retrofit levels. Additionally, the results of the NSGA-III multi-objective optimization and the top-ranked solutions for EE retrofit measures with their corresponding retrofit levels are presented. Section 4 provides main conclusions of this study.

2. Methodology

The methodology employed in this study applies multi-objective optimization to a specific category of buildings, aiming to minimize building energy consumption for heating, CO₂ emissions, and retrofit costs by considering various combinations of energy-efficient (EE) measures and retrofit levels. The selected building category represents a statistical sample of buildings constructed between 1970 and 1981, accounting for 24% of the total number of buildings in the housing stock and contributing to 38% of the energy required for heating the entire building stock (Arnautović-Aksić et al., 2016). This category of buildings incurs EE retrofit costs that are three to four times higher compared to other building categories such as multi-family houses, apartment buildings, or high rises (Kadrić et al., 2022b).

To establish the functional relationship between building energy consumption and key building parameters, the design of experiment (DOE) technique is employed (Sadeghifam et al., 2015; Kadrić et al., 2022a). A series of designed experiments is conducted to determine the correlation between building parameters and the system response. The Response Surface Methodology (RSM) is utilized to provide valuable information for building designers to identify the most influential parameters and optimize building design (Shao et al., 2014; García-Cuadrado et al., 2022). The selected building parameters reflect the impact of common EE retrofit measures implemented in the residential stock, such as installing thermal insulation on external walls and ceilings, replacing windows, and improving the existing heating system (Arnautović-Aksić et al., 2016).

Energy consumption modeling utilizing RSM indicates that the linear component of the model accounts for over 96% of the variation in specific final energy for heating (Kadrić et al., 2022a). Consequently, FFD methodology enables the fitting of a linear regression model and requires fewer simulations compared to

RSM, which is used in the current analysis. The developed model enables the prediction of energy consumption for heating and CO₂ emissions after implementing any combination of EE retrofit measures. Considering that the selected building type represents the majority of buildings in the total building stock, this study holds high relevance in the field of building energy efficiency.

The estimated cost of the selected EE retrofit measures employed in energy consumption modeling is determined using a bottom-up methodology (Kadrić et al., 2022b), which incorporates the cost of materials, equipment, labor, and other expenses. The cost of implementing each EE retrofit measure is divided into fixed and variable costs. The fixed cost is applied for each retrofit level, while the variable costs gradually increase with higher retrofit levels. For instance, the installation of thermal insulation on external walls can be performed at various levels with different insulation thicknesses, affecting the total costs. The cost analysis considers the fixed and variable costs associated with these measures and different levels of EE retrofit.

To determine the most effective EE retrofit measures, as well as their combinations and levels, that result in the lowest energy consumption, CO₂ emissions, and retrofit costs, multi-objective optimization techniques are employed. The non-dominated sorting genetic algorithm (NSGA-III) is utilized to solve the given multi-objective optimization problem. After implementing the composite desirability function, the study identifies the top ranked solutions and subsequently provides an economic analysis.

2.1. Building model

The calculation of building energy consumption is conducted using DesignBuilder software, which incorporates the EnergyPlus dynamic simulation module (US Department of Energy, 2022). Fig. 1(a) and (b) depict visual and thermographic representations, respectively, of the selected single-family home (SFH) building type constructed between 1971 and 1980, along with the DesignBuilder model.

The analyzed building consists of a ground floor, a first floor, and an unheated attic, as described in the national TABULA study (Arnautović-Aksić et al., 2016). The ground floor encompasses a bathroom, living room, kitchen, and hallway leading to the first floor, which comprises three bedrooms. In the DesignBuilder software, each room represents a separate temperature zone (European committee for standardization, 2019). The zone temperature, number of occupants, hourly occupancy rate, lighting schedule, electric equipment load, and working schedule align with our previous study (Kadrić et al., 2022a). The average number of residents per household, as well as data for model validation such as annual electrical energy consumption and annual final energy consumption for heating, are obtained from the Agency for Statistics B&H (Agic et al., 2016). The climatic data used in this study corresponds to the northern climatic region where the majority of buildings are situated (Arnautović-Aksić et al., 2016). To calculate the energy needed for heating, the EnergyPlus dynamic modeling tool is used. Eq. (1) is employed to determine the annual energy consumption for heating $E_{fin,H}$ (kWh/ann.) (Tootkaboni et al., 2021):

$$E_{fin,H} = Q_{H,nd} / \eta \quad (1)$$

where, $Q_{H,nd}$ (kWh/ann.) is annual energy need for heating and η (–) is overall heating system efficiency.

Eq. (2) is used to calculate the energy performance indicator (EP), specific final energy for heating EP_H (kWh/m² ann.) (Jovanović-Popović et al., 2013):

$$EP_H = E_{fin,H} / A_{H,net} \quad (2)$$



Fig. 1. (a) Visual and thermographic presentation of the selected building, (b) DesignBuilder model.

where $A_{H,net} = 65.4 \text{ m}^2$ is net heated area of the building.

Eq. (3) is employed to determine the annual CO_2 emission (kg/ann.) (Wang et al., 2017):

$$m_{\text{CO}_2} = EP_{H,n,\text{CO}_2} f_{n,\text{CO}_2} \quad (3)$$

where, $EP_{n,H}$ (kWh/ann.) is the same as above expressed for different energy carriers, and f_{n,CO_2} (kg/kWh) is GHG emission factor for delivered energy, expressed for energy carrier (n). No exported energy is analyzed in this study, therefore (3) is more simple than in Wang et al. (2017).

Eq. (4) is used to calculate the CO_2 emission indicator (EP_{CO_2}), specific CO_2 emission EP_{CO_2} ($\text{kg/m}^2 \text{ ann.}$):

$$EP_{\text{CO}_2} = m_{\text{CO}_2}/A_{H,net}. \quad (4)$$

2.2. Modeling of specific final energy consumption for heating and CO_2 emission

The primary aim of this study is to establish a correlation between different building parameters and the system response. To accomplish this objective, FFD methodology is employed. Compared to Response Surface Methodology (RSM) (Arnautović-Aksić et al., 2016; Jovanović-Popović et al., 2013), the FFD requires fewer simulations and allows for the fitting of a linear regression model. The developed model using this approach enables the calculation of energy consumption after implementing various combinations of EE retrofit measures. The FFD generates an experimental design matrix, which represents the individual simulation runs incorporating specific levels of pre-selected factors. This matrix is designed to include the optimal number of runs necessary to establish the relationship between the system response and factors. The FFD methodology facilitates the fitting of a linear regression model with cross-product terms of the independent factors, defined as follows:

$$y = \beta_0 + \sum_{i=1}^k \beta_i x_i + \sum_{i=1}^{k-1} \sum_{j=2}^k \beta_{ij} x_i x_j + \varepsilon \quad (5)$$

where y is the predicted system response, x_i and x_j are independent factors, β_0 , β_i and β_{ij} are intercept, linear, and interaction regression coefficients, respectively, k is the number of factors, and ε is random error.

In this study, data from regional national TABULA studies (Arnautović-Aksić et al., 2016; Jovanović-Popović et al., 2013) was utilized, and considering the most commonly implemented EE retrofit measures in B&H, four specific building design parameters were chosen for analysis to assess their influence on energy consumption and CO_2 emissions. These selected parameters are the heat transfer coefficient of external walls (A), the heat transfer coefficient of windows (B), the heat transfer coefficient of the ceiling (C), and the overall system efficiency (D). In the modeling of CO_2 emissions, the overall system efficiency, which is associated with the heating system, is combined with the GHG emission factor of the fuel used. Hence, factor D encompasses the combined

effect of the overall system efficiency and the fuel GHG emission factor for modeling CO_2 emissions. To evaluate the impact of EE retrofit measures, the values of these parameters are adjusted, encompassing a range of low to high energy-related properties. Table 1 provides a description of these building parameters (factors) along with their corresponding levels for conducting analysis of variance (ANOVA) and regression analysis.

An analysis of the country's energy statistics (Agic et al., 2016) indicates that a substantial percentage (86%) of households in the region depend on biomass and wood as their main fuel sources for heating systems. Coal (10.4%), electricity (2.19%), and natural gas (0.83%) are also utilized as alternative fuel sources, although to a lesser degree. The GHG emission factor for these fuels and energy sources is $0.0199 \text{ kg}_{\text{CO}_2}/\text{kWh}$ for biomass, $0.367 \text{ kg}_{\text{CO}_2}/\text{kWh}$ for coal, $0.793 \text{ kg}_{\text{CO}_2}/\text{kWh}$ for electricity, and $0.202 \text{ kg}_{\text{CO}_2}/\text{kWh}$ for natural gas (US Department of Energy, 2022). The given values are utilized to calculate the GHG emission factor for the low levels of the factors, representing the national energy mix, as presented in Table 1.

Table 2 displays the experimental matrix generated using FFD, which presents the computed annual energy consumption for heating, specific final energy for heating, and specific CO_2 emission. The total number of simulation runs conducted is 16. The specific final energy for heating EP_H , values range from a maximum of $278.3 \text{ kWh/m}^2 \text{ ann.}$ for low energy-related properties to a minimum of $17.9 \text{ kWh/m}^2 \text{ ann.}$ for high energy-related properties. The specific CO_2 emission EP_{CO_2} values vary from a maximum of $20.8 \text{ kg/m}^2 \text{ ann.}$ for low energy-related properties to a minimum of $0.4 \text{ kg/m}^2 \text{ ann.}$ for high energy-related properties. It is worth noting that, as per the country's energy statistics (Agic et al., 2016), the average CO_2 emission per heated surface area for households in B&H is $18.93 \text{ kg/m}^2 \text{ ann.}$, derived from the country's average GHG emission factor and total surface area of SFH (Arnautović-Aksić et al., 2016).

2.3. Cost of EE retrofit measures

The costs related to the implementation of EE retrofit measures are determined using a bottom-up methodology, which takes into account the costs of materials, equipment, labor, and other applicable expenses. The following equation is utilized to calculate the total costs of implementing an EE retrofit measure (Kadrić et al., 2022b):

$$C_{\text{meas}} = (C_{\text{mat}} + C_{\text{lab}} + C_{\text{gen}})(1 + \text{VAT}) \quad (6)$$

where, C_{mat} are the materials and equipment with all connected costs in Euro €, C_{lab} are labor and all connected costs in Euro €, C_{gen} are general expenses € and VAT is Value Added Tax (%).

During the evaluation of each EE measure implementation, labor engagement is carefully assessed in accordance with construction and mechanical standards. Additionally, material requirements are determined based on the specific characteristics of the building undergoing retrofit, such as the dimensions of

Table 1
Description of building parameters (factors) and their respective levels for ANOVA and regression analysis.

Factor	Low level (−1)	High level (+1)
A: External wall heat transfer coefficient U_{wall} (W/m ² K)	No thermal insulation ($\delta_{T1} = 0$ cm) 2.01	With thermal insulation ($\delta_{T1} = 20$ cm) 0.18
B: Windows heat transfer coefficient U_{win} (W/m ² K)	Wooden frame with single glazing 5.00	PVC frame/Triple glazing/Low-E, Argon filled 0.96
C: Ceiling heat transfer coefficient U_{ceil} (W/m ² K)	No thermal insulation ($\delta_{T1} = 0$ cm) 1.75	With thermal insulation ($\delta_{T1} = 25$ cm) 0.14
D: Overall system efficiency η (%) GHG emission factor f_{CO_2} (kg/kWh)	Solid fuel-burning stove 50 0.075	Central heating - high efficiency 95 0.019

Table 2
The experimental matrix and simulated energy consumption for heating and CO₂ emission.

Run	Factor values (coded)				Simulated values		
	A	B	C	D	EF_H (kWh/ann.)	EP_H (kWh/m ² ann.)	EP_{CO_2} (kg/m ² ann.)
1	−1	−1	−1	−1	18 198	278.3	20.8
2	1	−1	−1	−1	8 018	122.6	9.1
3	−1	1	−1	−1	15 085	230.7	17.2
4	1	1	−1	−1	5 158	78.9	5.9
5	−1	−1	1	−1	14 936	228.4	17.0
6	1	−1	1	−1	4 624	70.7	5.3
7	−1	1	1	−1	11 978	183.2	13.7
8	1	1	1	−1	2 224	34.0	2.5
9	−1	−1	−1	1	10 110	146.4	2.9
10	1	−1	−1	1	4 455	64.5	1.3
11	−1	1	−1	1	8 381	121.4	2.4
12	1	1	−1	1	2 866	41.5	0.8
13	−1	−1	1	1	8 298	120.2	2.4
14	1	−1	1	1	2 569	37.2	0.7
15	−1	1	1	1	6 655	96.4	1.9
16	1	1	1	1	1 235	17.9	0.4

the external walls and ceiling, and the quantity and dimensions of windows, among others (European committee for standardization, 2019). The analysis also takes into consideration various tasks involved in the retrofit process, including demolition, assembly, installation, and disposal of materials and equipment. Material and equipment cost is calculated as follows:

$$C_{mat} = \sum_{i=1}^n q_i u_i \tag{7}$$

q_i is the quantity of the i^{th} component installed and used during the construction, and u_i is the corresponding unit cost of the i^{th} component (€/component).

When estimating labor costs, several factors are considered, including the time required to complete each task, the qualifications of the workers involved, and the average salary corresponding to those qualifications (Bosnia and Herzegovina Agency for Statistic, 2022a). The total labor cost is determined by breaking down the implementation of the measure into multiple tasks, and it can be calculated using the following expression:

$$C_{lab} = 1.7C_{lab,nett} = 1.7 \sum_{i=1}^n T_i L_i W_i \tag{8}$$

where, $C_{lab,nett}$ is the labor cost after tax (€), T_i is the quantity of work for the specific task i , L_i is the working norm required per unit of T_i (hours/task), and W_i is the average wage (€/hours) based on the required labor qualification level.

The qualifications of workers range from semi-skilled to skilled, according to the standards specified for each task (Bucar, 2003). The total number of working hours is calculated

by summing up the time spent and work completed for each task, taking into account the professional qualifications required for each task. The labor cost and total working hours are then determined by adding up the costs for each task and multiplying the sum by a coefficient of 1.7, representing the gross to net costs (salary). General expenses, including the depreciation of fixed assets, investments, ongoing maintenance of fixed assets, salaries for overhead employees, field allowances, and business profit, are all considered. Additionally, the value-added tax (VAT) at a rate of 17% is calculated, along with the total expenditures for implementing the EE retrofit measure using Eq. (6). The methodology presented allows for an accurate determination of the total cost of EE retrofit measures, considering various factor levels. At factor level (−1), where no EE retrofit measure is implemented, the total cost for all measures is zero. However, it is important to note that even at very low levels of EE retrofit, such as (−0.99), fixed costs, including materials, labor, and general charges, are still incurred. These fixed costs remain constant across all retrofit levels, while additional expenses are incurred for more extensive retrofits. Therefore, with the exception of level (−1), each retrofit level incurs fixed costs, while the variable costs gradually increase with a more extensive retrofit. This comprehensive approach accounts for the costs incurred at different retrofit levels, providing valuable insights for decision-makers and stakeholders evaluating EE retrofit strategies. The total cost of combined EE retrofit measures is determined by summing up the costs of each EE measure $C_{meas,j}$:

$$C_t = \sum_{j=1}^4 C_{meas,j} \tag{9}$$

Total costs are computed for all combinations of factor values in the range of -1 to $+1$.

2.4. Multi-objective optimization using genetic algorithm

The objectives of building retrofit optimization are to minimize the specific final energy for heating (EP_H) and the specific CO_2 emissions (EP_{CO_2}) while achieving the minimum total cost of EE retrofit measures (C_t). However, these objectives exhibit contrasting trends as more extensive EE retrofit measures are implemented. Specifically, the specific final energy for heating and specific CO_2 emissions decrease, indicating improved energy efficiency and reduced environmental impact. On the other hand, the total cost of EE retrofit measures increases with the implementation of more comprehensive retrofit measures.

The optimization of these objectives is dependent on four factors: the external wall heat transfer coefficient (A), windows heat transfer coefficient (B), ceiling heat transfer coefficient (C), and the overall system efficiency coupled with the GHG emission factor (D). Multi-objective optimization problem, mathematically is defined as follows:

$$\begin{aligned} & \min_{A,B,C,D} EP_H \\ & \min_{A,B,C,D} EP_{CO_2} \\ & \min_{A,B,C,D} C_t \end{aligned} \tag{10}$$

subject to:

$$\begin{aligned} -1 & \leq A \leq 1 \\ -1 & \leq B \leq 1 \\ -1 & \leq C \leq 1 \\ -1 & \leq D \leq 1 \end{aligned} \tag{11}$$

In order to tackle the multi-objective optimization problem described by Eqs. (10) and (11), we have employed genetic algorithms (GA) as our optimization approach. GA is a type of evolutionary algorithm known for its adaptability and versatility in solving a wide range of optimization problems, including building retrofit optimization in various domains (Sharif and Hammad, 2019; Ascione et al., 2019; Roberti et al., 2017; Rosso et al., 2017). While GA is a heuristic algorithm, it excels at generating solutions that are near-optimal, meaning they are sufficiently good, even if not guaranteed to be optimal.

To solve the multi-objective optimization problem, we have utilized the NSGA-III genetic algorithm (Deb and Jain, 2013), which builds upon its well-established predecessor, NSGA-II, inheriting its beneficial mechanisms and features (Emmerich and Deutz, 2018). The key advantage of NSGA-III over NSGA-II lies in its improved capability to handle multiple objectives, ensuring a more enhanced distribution of solutions. Instead of using crowding distance as in NSGA-II, NSGA-III employs the concept of reference points. Through adaptive addition and removal of a predefined set of well-distributed reference points, NSGA-III achieves better partitioning of the objective space, resulting in improved spread and distribution of solutions across the objective space (Ishibuchi et al., 2016).

By executing the NSGA-III algorithm, we obtain a set of solutions that represent the Pareto front. This Pareto front comprises all the non-dominated solutions, meaning that no solution on the Pareto front is better than any other solution in terms of all objectives. Therefore, the Pareto front obtained through NSGA-III provides a comprehensive representation of the trade-offs and optimal solutions for our multi-objective optimization problem.

2.5. Desirability function and selection of best solutions

In order to handle the large number of non-dominated solutions and assist decision-makers in selecting the most preferable options based on their preferences, various methods can be employed. One such method is the use of multi-criteria decision analysis techniques like TOPSIS (Mostafazadeh et al., 2023; Pinzon Amorocho and Hartmann, 2022). These methods allow for the ranking of solutions based on decision-makers' preferences. Another approach is to utilize the desirability function (DF), commonly used in the design of experiments for multi-objective optimization (Harrington, 1965; Derringer and Suich, 1980).

The desirability function transforms multiple objective functions, which may be measured on different scales, into a scale-free value normalized between 0 and 1. By applying the DF, a higher value indicates a better solution, while a lower value indicates a less desirable solution. In our study, we propose using the DF method to rank the non-dominated solutions. Since each objective function in our study (EP_H , EP_{CO_2} and C_t) is to be minimized, the DF for each objective can be defined as follows:

$$d_i = \begin{cases} 1 & y_i < T_i \\ \left(\frac{U_i - y_i}{U_i - T_i}\right)^{s_i} & T_i < y_i < U_i \\ 0 & y_i > U_i \end{cases} \tag{12}$$

where T_i is the target value of the objective (lower limit), U_i is the upper limit of the objective, y_i is objective value, and s_i is the weight of each objective.

The assignment of weights, denoted as s_i , in the desirability function reflects the decision-maker's preferences or priorities. These weights can be determined through subjective judgments, expert opinions, or objective statistical methods. The weights s_i can take on values of 1 or can be greater or less than 1, depending on the desired emphasis on a particular objective.

When s_i is set to 1, the desirability function becomes linear, indicating equal importance given to each objective. On the other hand, when s_i is greater than 1 or less than 1, more or less emphasis is placed on a specific target, respectively.

Once the individual desirability functions, denoted as d_i , for multiple objectives have been established, they are combined into a composite desirability function, denoted as CD . The composite desirability function is calculated as the geometric mean of the individual desirability functions. Mathematically, it can be expressed as follows:

$$CD = (d_1 \times d_2 \times \dots \times d_n)^{\frac{1}{n}} = \left(\prod_{i=1}^n d_i\right)^{\frac{1}{n}} \tag{13}$$

where CD is composite desirability, d_i is the desirability function of individual objectives, n is the number of objectives. The composite desirability function, CD , provides an aggregated measure of the overall desirability of a solution, taking into account the preferences assigned to each objective. By evaluating the composite desirability function, decision-makers can identify the solutions that best align with their priorities and make informed choices accordingly.

2.6. Cost-effectiveness analysis

To assess the economic feasibility of different EE retrofit levels, a comprehensive cost analysis is performed, taking into account both the upfront investment costs and the potential energy cost savings. The evaluation is primarily focused on determining the Simple Payback Period (SPP), which quantifies the time required to recover the initial investment costs C_t through the anticipated annual energy cost savings C_{sav} .

Table 3
ANOVA for the specific final energy for heating EP_H model.

Source	DF	SS	Contribution	Adj SS	Adj MS	F-Value	p-Value
Model	10	92 174.6	99.99%	92 174.6	9 217.5	6 710.07	0.000
Linear	4	85 898.4	93.18%	85 898.4	21 474.6	15 632.94	0.000
A. U_{wall}	1	54 939.2	59.60%	54 939.2	54 939.2	39 994.29	0.000
B. U_{win}	1	4 370.2	4.74%	4 370.2	4 370.2	3 181.38	0.000
C. U_{ceil}	1	5 488.9	5.95%	5 488.9	5 488.9	3 995.78	0.000
D. η	1	21 100.1	22.89%	21 100.1	21 100.1	15 360.31	0.000
2-way interactions	6	6 276.2	6.81%	6 276.2	1 046.0	761.49	0.000
A · B. $U_{wall} \cdot U_{win}$	1	22.3	0.02%	22.3	22.3	16.25	0.010
A · C. $U_{wall} \cdot U_{ceil}$	1	0.1	0.00%	0.1	0.1	0.04	0.850
A · D. $U_{wall} \cdot \eta$	1	5 291.4	5.74%	5 291.4	5 291.4	3 852.01	0.000
B · C. $U_{win} \cdot U_{ceil}$	1	12.9	0.01%	12.9	12.9	9.38	0.028
B · D. $U_{win} \cdot \eta$	1	420.9	0.46%	420.9	420.9	306.41	0.000
C · D. $U_{ceil} \cdot \eta$	1	528.7	0.57%	528.7	528.7	384.85	0.000
Error	5	6.9	0.01%	6.9	1.4		
Total	15	92 181.5	100.00%				

DF – degrees of freedom; SS – the sum of squares; Adj SS – the adjusted sum of squares; Adj MS – adjusted mean squares.

The simple payback period is calculated by dividing the initial investment costs C_t by the estimated annual energy cost savings C_{sav} :

$$SPP = C_t / C_{sav} \quad (14)$$

The calculation of the average price of final energy for households incorporates data obtained from the country's energy statistics (Agic et al., 2016), along with the average prices of energy and fuel. The input values considered are the respective proportions of fuel in the country's energy mix, which consist of 86% biomass and wood, 10.4% coal, 2.19% electricity, and 0.83% natural gas. Additionally, the corresponding average costs of final energy are taken into account.

Based on available information, the average cost of final energy for biomass and wood is determined to be 0.057 €/kWh, while for coal it is 0.032 €/kWh. The average cost of final energy for electricity is calculated to be 0.076 €/kWh, and for natural gas, it is determined as 0.068 €/kWh (Bosnia and Herzegovina Agency for Statistic, 2022b). As a result of these considerations, the average baseline cost of final energy for households is established at 0.055 €/kWh. This value serves as a reference for evaluating the cost-effectiveness of energy efficiency retrofit measures and estimating potential energy cost savings.

3. Results

3.1. Analysis of specific final energy for heating and CO_2 emission models

The model for predicting the specific final energy for heating (EP_H) was developed using DesignExpert software, incorporating the simulated values of specific final energy for heating as presented in Table 2. The model is defined as follows:

$$EP_H = 117.014 - 58.598 A - 16.527 B - 18.522 C - 36.315 D + 1.181 A B + 0.058 A C + 18.186 A D + 0.897 B C + 5.129 B D + 5.748 C D \quad (15)$$

The model for predicting the specific CO_2 emission (EP_{CO_2}) was developed using DesignExpert software, utilizing the simulated values of specific CO_2 emission as depicted in Table 2. The model is defined as follows:

$$EP_{CO_2} = 6.5249 - 3.2675 A - 0.9216 B - 1.0328 C - 4.9124 D + 0.0659 A B + 0.0033 A C + 2.4600 A D + 0.0500 B C + 0.6938 B D + 0.7776 C D \quad (16)$$

The analysis of variance (ANOVA) is employed to evaluate the statistical significance of the factors and their interactions on system responses. By examining the F -values and their corresponding p -values, the significance of the effects of factors and interactions can be determined. The statistical tests are conducted at a significance level of $\alpha = 0.05$, allowing for an assessment of the level of significance in the observed results.

Table 3 presents the ANOVA results for the specific final energy for the heating EP_H model. The table includes information such as degrees of freedom, sum of squares, factor contributions, adjusted sum of squares, adjusted mean squares, and F and p values. The model used for predicting EP_H is statistically significant ($p < 0.05$), as are its linear and 2-way interaction components ($p < 0.05$). All terms of the model (linear and 2-way interactions) except AC are statistically significant ($p < 0.05$). The contribution analysis reveals that the linear component accounts for 93.18% of the variations in EP_H , while the 2-way interactions component explains 6.81%. Among the factors, the most influential one is the external wall heat transfer coefficient U_{wall} (A), which contributes 59.60% to explaining the variations in EP_H . The heating system efficiency η and the fuel GHG emission factor f_{CO_2} (D) follow, with a contribution of 22.89%. The interaction term AD contributes 5.74%. On the other hand, the ceiling heat transfer coefficient U_{ceil} (C) and the windows heat transfer coefficient U_{win} (B) are the least influential factors, with contributions of 5.95% and 4.74%, respectively. These findings align with the main effect plot of the factors shown in Fig. 2.

Table 4 presents the ANOVA results for the specific CO_2 emission EP_{CO_2} model. The model used to predict EP_{CO_2} is statistically significant, including its linear and 2-way interaction components ($p < 0.05$). All main effects and 2-way interactions involving D in the model are statistically significant ($p < 0.05$).

The contribution analysis reveals that the linear component accounts for 83.70% of the variations in EP_{CO_2} , while the 2-way interactions component explains 16.28%. Among the factors, the results indicate that D, which represents the combined effect of the heating system efficiency η and fuel GHG emission factor f_{CO_2} , is the most influential factor, contributing 55.0% to explaining the variations in EP_{CO_2} . Following D is A, representing the external wall heat transfer coefficient U_{wall} , with a contribution of 24.33%, and the interaction term AD with a contribution of 13.79%. Factors C and B, representing the ceiling heat transfer coefficient U_{ceil} and windows heat transfer coefficient U_{win} , respectively, have the least influence, with contributions of 2.43% and 1.94%, respectively. These findings align with the main effect plot of the factors shown in Fig. 2.

The models' performance in predicting the responses is evaluated using adjusted R^2 (R^2_{adj}) and predicted R^2 (R^2_{pred}). For the

Table 4
ANOVA for the specific CO₂ emission EP_{CO_2} model.

Source	DF	SS	Contribution	Adj SS	Adj MS	F-Value	p-Value
Model	10	701.902	99.99%	701.902	70.190	4 524.69	0.000
Linear	4	587.590	83.70%	587.590	146.897	9 469.49	0.000
A. U_{wall}	1	170.825	24.33%	170.825	170.825	11 011.95	0.000
B. U_{win}	1	13.588	1.94%	13.588	13.588	875.95	0.000
C. U_{ceil}	1	17.067	2.43%	17.067	17.067	1 100.19	0.000
D. η	1	386.109	55.00%	386.109	386.109	24 889.85	0.000
2-way interactions	6	114.313	16.28%	114.313	19.052	1 228.16	0.000
A · B. $U_{wall} \cdot U_{win}$	1	0.069	0.01%	0.069	0.069	4.47	0.088
A · C. $U_{wall} \cdot U_{ceil}$	1	0.000	0.00%	0.000	0.000	0.01	0.921
A · D. $U_{wall} \cdot \eta$	1	96.827	13.79%	96.827	96.827	6 241.79	0.000
B · C. $U_{win} \cdot U_{ceil}$	1	0.040	0.01%	0.040	0.040	2.58	0.169
B · D. $U_{win} \cdot \eta$	1	7.702	1.10%	7.702	7.702	496.51	0.000
C · D. $U_{ceil} \cdot \eta$	1	9.674	1.38%	9.674	9.674	623.61	0.000
Error	5	0.078	0.01%	0.078	0.016		
Total	15	701.980	100.00%				

DF – degrees of freedom; SS – sum of squares; Adj SS – adjusted sum of squares; Adj MS – adjusted mean squares.

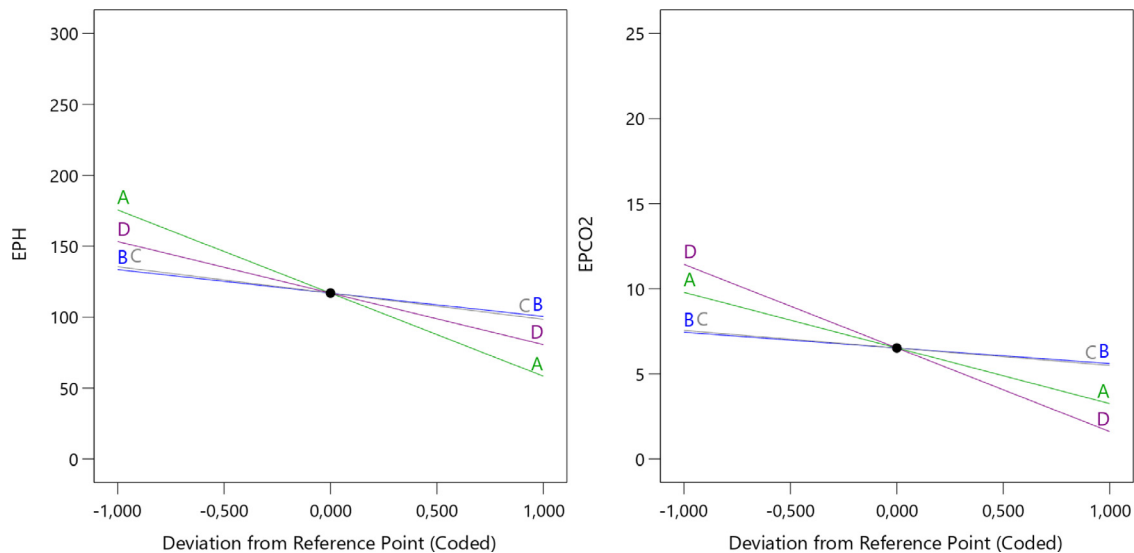


Fig. 2. Main effect plot for the specific final energy for heating and specific CO₂ emission.

EP_H model, the coefficients R^2_{adj} and R^2_{pred} are 99.98% and 99.92% respectively, indicating a strong agreement between the model-predicted and simulated data. Similarly, for the EP_{CO_2} model, the coefficients R^2_{adj} and R^2_{pred} are 99.97% and 99.89% respectively, demonstrating the adequacy of the models in predicting EP_H and EP_{CO_2} .

Fig. 2 displays the main effects plot for EP_H and EP_{CO_2} . In this plot, the response is plotted against the lower and upper limits of each design factor, illustrating the relationship between the factors and the corresponding responses.

The external wall heat transfer coefficient (A) has the largest impact on EP_H . Changing the value of A from -1 to $+1$, corresponding to a change in value from 2.01 to 0.18 W/m² K, results in a significant reduction in EP_H . This is because in the studied single-family house (SFH), which has a low window-to-wall ratio of only 10%, a significant portion of the external walls is exposed to the environment, making them a major source of transmission losses before renovation. The overall heating system efficiency (D) is the second most influential factor on EP_H . Changing D from -1 to $+1$, representing a change in system efficiency from the lowest value of 50% to the highest value of 90%, leads to a significant reduction in EP_H . On the other hand, the impact of the heat transfer coefficient of the ceiling below the unheated attic (C) and the windows (B) on EP_H is relatively lower.

For EP_{CO_2} , the external wall heat transfer coefficient (A) has the largest impact. The combined effect of the overall heating

system efficiency and the fuel GHG emission factor (D) is the second most influential factor on EP_{CO_2} . The impact of the heat transfer coefficient of the ceiling below the unheated attic (C) and the windows (B) on EP_{CO_2} is relatively lower.

Overall, the findings highlight the significance of improving the external wall insulation and enhancing the heating system efficiency in reducing both EP_H and EP_{CO_2} in the studied SFH.

The combined influence of the two most influential factors, A and D, along with their interaction AD, on the variables EP_H and EP_{CO_2} , is depicted through a 3D surface plot in Fig. 3. The highest values of EP_H and EP_{CO_2} are observed when both factors are set to a low level (-1). As the factors are increased from -1 to $+1$, there is a significant linear decrease in both responses. The lowest values of EP_H and EP_{CO_2} are observed when both factors are at a high level ($+1$). Thus, in order to minimize EP_H , it is necessary to decrease U_{wall} to 0.18 W/m² K and increase the overall system efficiency η to 95%. Similarly, to minimize EP_{CO_2} , it is required to decrease U_{wall} to 0.18 W/m² K, increase the overall system efficiency η to 95%, and reduce the GHG emission factor f_{CO_2} to 0.019 kg/kWh.

3.1.1. Model validation

The model used to predict building energy consumption, as defined by Eq. (15), is validated using data reported from a national-scale survey that covered 7083 households in B&H (Agic

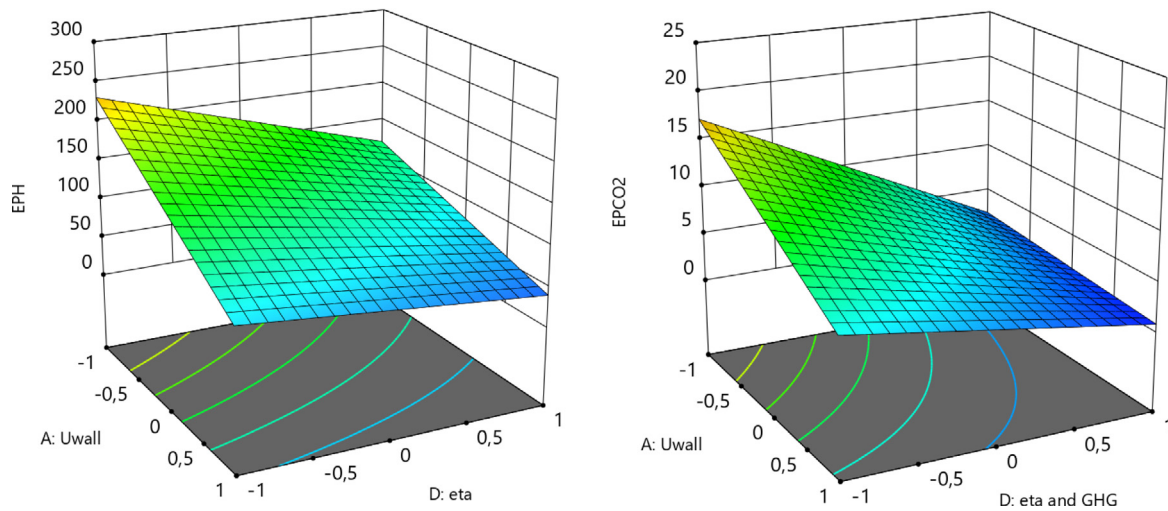


Fig. 3. 3D response surface plot of EP_H (left) and EP_{CO_2} (right) as a function of A and D.

et al., 2016). According to the survey findings, the average annual consumption of wood for space heating per household is approximately 7.7 m^3 . To calculate the final energy consumption for heating, the fuel quantity consumed is multiplied by the respective lower calorific values. On average, the lower calorific value for wood is 1950 kWh/m^3 (Neufert and Neufert, 2012), and the specific annual final energy consumption for wood-based heating systems is $230 \text{ kWh/m}^2 \text{ ann}$.

To validate the model, the building envelope heat transfer coefficients are adjusted to national typical values for SFH (single-family homes), as provided in the national TABULA study (Arnautović-Aksić et al., 2016). Specifically, the external wall heat transfer coefficient is set to $1.64 \text{ W/m}^2 \text{ K}$, the ceiling heat transfer coefficient to $1.75 \text{ W/m}^2 \text{ K}$, and the windows are double glazed with a wood frame, having a heat transfer coefficient of $3.0 \text{ W/m}^2 \text{ K}$. The dominant heating system in these households is a single stove, wood-based system, which has an overall efficiency of 50% (Carvalho et al., 2016). By applying Eq. (15) and utilizing the coded factor values ($A = -0.5956$, $B = -0.0099$, $C = -1$, and $D = -1$), the calculated specific final energy is $223.6 \text{ kWh/m}^2 \text{ ann}$. This value is in good agreement with the annual specific final energy for heating of households in B&H, which is $230 \text{ kWh/m}^2 \text{ ann}$.

3.2. Analysis of EE retrofit measures cost

Fig. 4 illustrates the cost structure associated with the installation of thermal insulation on external walls, denoted as $C_{\text{meas},A}$, with the aim of providing a clear understanding of the included costs. This cost structure is presented for three different levels of retrofitting: low, middle, and high. Across all retrofit levels, certain costs such as general expenses and labor costs remain constant. The material cost remains constant when implementing the low retrofit level (-0.99). However, as deeper retrofits are implemented, the required materials become more expensive, resulting in an overall increase in the total cost of the measure. The total cost across the entire range of retrofit levels can be represented as the sum of fixed costs, which include general expenses, labor costs, and material costs at the lowest retrofit level, and variable costs, which encompass the additional expenses associated with installing more efficient and higher quality materials and equipment.

Fig. 5 presents the total costs of four energy-efficient (EE) retrofit measures, namely $C_{\text{meas},A}$, $C_{\text{meas},B}$, $C_{\text{meas},C}$ and $C_{\text{meas},D}$, across different retrofit levels ranging from -1 to $+1$. The total

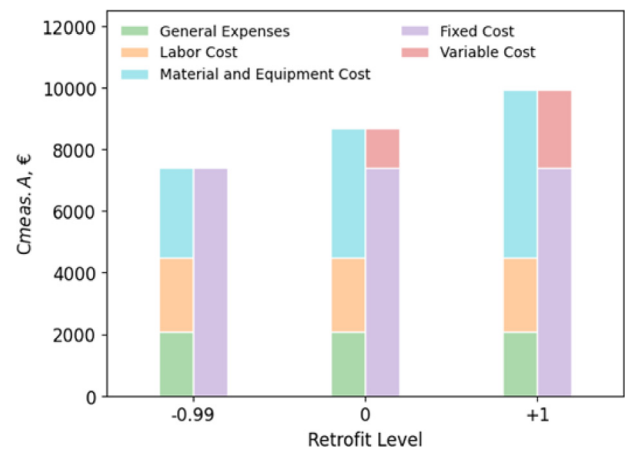


Fig. 4. $C_{\text{meas},A}$ cost structure (installing thermal insulation on external walls).

cost of each EE retrofit measure comprises fixed and variable components. The fixed cost remains constant throughout the entire range of retrofit levels, regardless of the specific level. On the other hand, the variable cost increases linearly as deeper retrofit measures are implemented and reaches its maximum at retrofit level $+1$. At retrofit level -1 , where no retrofit measure is implemented, the total cost of the measure is equal to 0. Implementing any retrofit measure from level -0.99 to $+1$ results in an increase in the total cost.

The contribution of the fixed cost to the total cost is relatively high at lower retrofit levels and gradually decreases at higher retrofit levels, generally ranging between 60% and 84%. This indicates the importance of implementing more extensive building retrofits to leverage both fixed and variable costs and achieve greater energy and CO_2 emission performance improvements.

Analyzing all four considered EE retrofit measures, it is evident that the installation of thermal insulation on external walls $C_{\text{meas},A}$ has the highest total cost. This measure affects the external wall heat transfer coefficient (A), and at retrofit level $+1$, the total cost amounts to 9939 €. The second-highest total cost is associated with the installation of a central heating system $C_{\text{meas},D}$, which impacts the overall heating system efficiency and fuel GHG emission factor (D). At retrofit level $+1$, the total cost of implementing this measure is 6374 €. The retrofit measure for windows replacement $C_{\text{meas},B}$, affecting the windows' heat transfer coefficient (B),

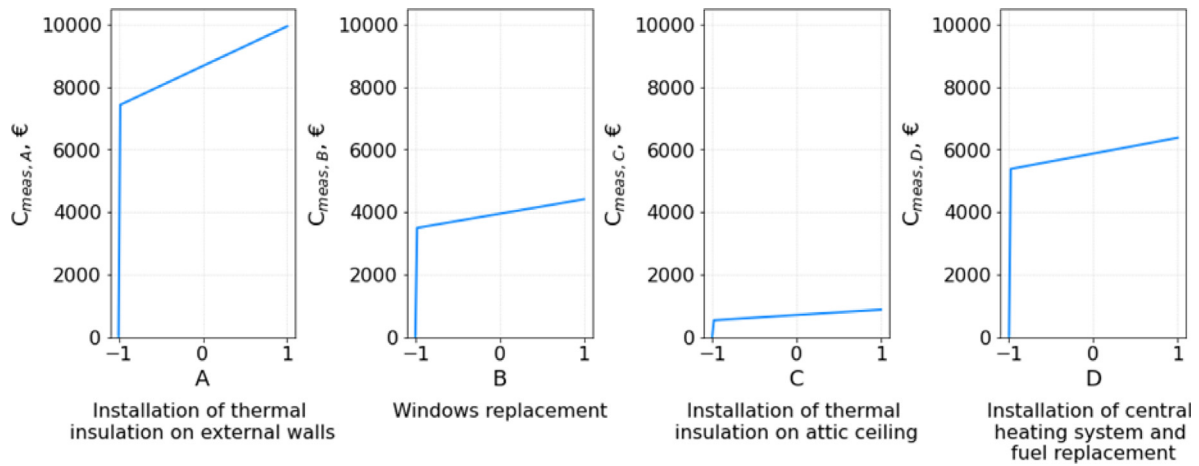


Fig. 5. EE retrofit measures total costs.

follows with a total cost of 4407 € at retrofit level +1. Lastly, the installation of thermal insulation on the attic ceiling $C_{meas.C}$, which impacts the ceiling heat transfer coefficient (C), has the lowest total cost of 876 € at retrofit level +1.

EE retrofit measures total costs $C_{meas.A}$, $C_{meas.B}$, $C_{meas.C}$ and $C_{meas.D}$ for different retrofit levels (-1 to +1) are calculated as follows:

$$C_{meas.A} = \begin{cases} 0 & A = -1 \\ 7402.64 + 1268.22(1 + A) & -0.99 \leq A \leq +1 \end{cases} \quad (17)$$

$$C_{meas.B} = \begin{cases} 0 & B = -1 \\ 3482.53 + 462.65(1 + B) & -0.99 \leq B \leq +1 \end{cases} \quad (18)$$

$$C_{meas.C} = \begin{cases} 0 & C = -1 \\ 534.62 + 170.81(1 + C) & -0.99 \leq C \leq +1 \end{cases} \quad (19)$$

$$C_{meas.D} = \begin{cases} 0 & D = -1 \\ 5367.69 + 503.02(1 + D) & -0.99 \leq D \leq +1 \end{cases} \quad (20)$$

3.3. Multi-objective optimization

The multi-objective optimization problem, as defined in Section 2.4, is solved using the NSGA-III genetic algorithm. Upon executing the NSGA-III algorithm, a set of non-dominated solutions, also known as the Pareto front, is obtained. Figs. 6 and 7 display the theoretical solution space, NSGA-III population space, Pareto front, and the top five ranked solutions. The theoretical solution space is obtained by varying all factor values within the range of -1 to +1, using Eqs. (15) to (20). Since the components of the total cost of combined EE retrofit measures (C_t) are defined as piecewise-linear functions (17)–(20), the solution space is discrete and discontinuous.

The NSGA-III population space and Pareto front are obtained after 100 generations with a population size of 500. The algorithm converges to a Pareto front consisting of 24 solutions (individuals). The ranking of solutions in the Pareto front is achieved using the composite desirability function (13), with weights of 6, 3, and 1 assigned to objectives EP_H , EP_{CO_2} and C_t , respectively. These weights prioritize building retrofits that lead to a high energy class classification with low energy consumption, in line with the recommendations in the “Rulebook on minimum requirements for energy performance of buildings” (Official Gazette of Federation of Bosnia and Herzegovina, 2019).

The total cost of the combined EE retrofit measures (C_t) for the solutions in the Pareto front ranges from 0 €, with $EP_H = 278.20$ kWh/m² ann and $EP_{CO_2} = 20.70$ kg/m² ann., to 21597 €, with $EP_H = 19.25$ kWh/m² ann. and $EP_{CO_2} = 0.44$ kg/m² ann.

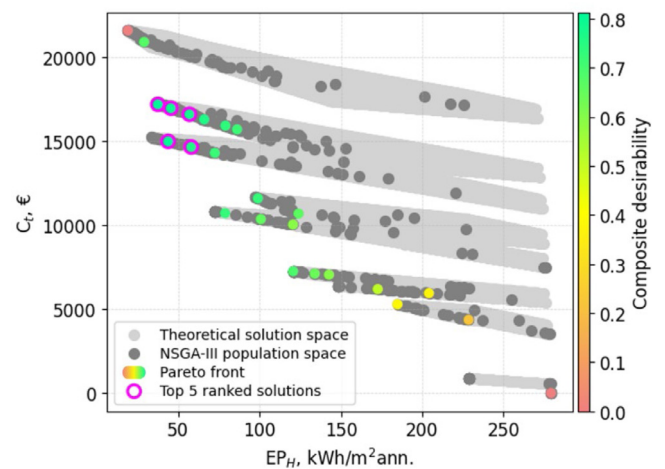


Fig. 6. NSGA-III optimization results projected on $EP_H C_t$ plane.

These anchor solutions represent the extreme points with the lowest composite desirability function value of 0 (highlighted as red points in Figs. 6 and 7). Anchor solutions either have the maximum EP_H and EP_{CO_2} values and the minimum C_t value or vice versa. Other objectives of the Pareto front solutions are partially satisfied, falling between the minimum and maximum objective values. The top five ranked solutions possess the highest composite desirability function values, ranging from 0.76 to 0.81. These solutions are extensively discussed in detail in Section 3.4.

3.4. Pareto front solutions ranking

The developed methodology and conducted analysis allow for the determination of the most favorable solutions, which encompass energy efficiency retrofit measures and retrofiting levels. These solutions are ranked based on composite desirability functions, where higher values indicate better solutions. Figs. 6 and 7, display the non-dominated solutions with their composite desirability function values. Additionally, these solutions are listed in Table 5. where solutions 23 and 24 represents anchor solutions. Each solution includes optimal building parameters (measures to be implemented), along with their respective EP_H , EP_{CO_2} , C_t values, and composite desirability function.

Table 5 presents the non-dominated solutions, which encompass all the considered energy efficiency (EE) retrofit measures:

Table 5
Non-dominated solutions ranked by composite desirability (CD) function.

Rank	Building parameters (coded)				Objective function values			CD ^a	
	A	B	C	D	EP _H	EP _{CO2}	C _t		
	(-)	(-)	(-)	(-)	(kWh/m ² ann.)	(kg/m ² ann.)	(Eur.)	(-)	
Baseline	-1.00	-1.00	-1.00	-1.00	278.2	20.7	0.0	-	
1	1.00	-1.00	1.00	1.00	37.7	0.7	17 189.1	0.81	
2	1.00	0.47	1.00	-1.00	44.0	3.2	14 979.8	0.80	
3	1.00	-1.00	1.00	0.54	45.7	1.7	16 959.5	0.79	
4	0.53	-1.00	1.00	1.00	57.1	1.1	16 596.2	0.78	
5	1.00	-0.25	1.00	-1.00	58.1	4.3	14 643.4	0.76	
6	1.00	-1.00	-1.00	0.96	66.2	1.4	16 294.0	0.76	
7	0.00	-1.00	1.00	1.00	79.2	1.5	15 921.6	0.74	
8	0.92	-1.00	1.00	-1.00	79.0	5.9	10 712.6	0.73	
9	-1.00	0.87	1.00	1.00	99.2	2.0	11 596.2	0.73	
10	1.00	-1.00	1.00	-1.00	72.7	5.4	14 297.9	0.72	
11	0.54	-1.00	-1.00	0.94	86.3	2.0	15 702.6	0.72	
Non-dominated solutions	12	-1.00	-1.00	1.00	1.00	120.8	2.4	7 250.0	0.69
	13	1.00	1.00	1.00	-0.38	29.2	20 904.0	0.68	
	14	-1.00	0.79	-1.00	1.00	124.1	2.4	10 683.7	0.66
	15	0.64	-1.00	1.00	-1.00	100.9	7.5	10 355.6	0.66
	16	-1.00	-1.00	0.56	0.87	134.0	3.5	7 110.4	0.64
	17	-1.00	-1.00	1.00	0.59	142.8	5.4	7 044.4	0.60
	18	0.38	-1.00	1.00	-1.00	120.7	9.0	10 034.1	0.59
	19	-1.00	-1.00	-1.00	0.63	172.7	6.3	6 186.7	0.51
	20	-1.00	1.00	1.00	-1.00	184.9	13.7	5 284.1	0.38
	21	-1.00	-1.00	-1.00	0.15	204.2	10.6	5 944.7	0.37
	22	-1.00	-1.00	1.00	-1.00	228.5	17.0	4 358.8	0.22
	23	-1.00	-1.00	-1.00	-1.00	279.2	20.7	0.0	0.00
	24	1.00	1.00	1.00	1.00	19.2	0.4	21 596.9	0.00

^a CD = Composite desirability.

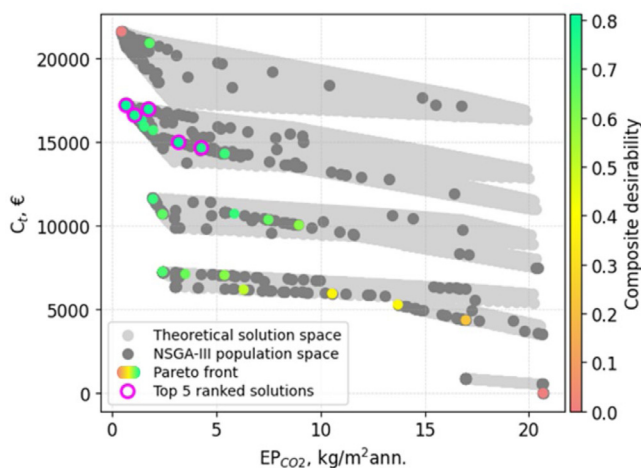


Fig. 7. NSGA-III optimization results projected on EP_{CO2}C_t plane.

installing thermal insulation on external walls (A) and unheated attic ceiling (C), replacing windows (B), and implementing a central heating system along with reducing the fuel GHG emission factor (D).

For the top five ranked solutions the algorithm generally suggests implementing high levels of thermal insulation on external walls and attic ceilings across the obtained solutions, while the implementation levels of the other two measures vary.

Among the measures included in top five ranked solutions, the installation of thermal insulation on external walls provides the largest reduction in EP_H and the second-largest reduction in EP_{CO2}. Despite having the highest implementation cost, the algorithm recommends implementing it at a high level (+1). On the other hand, the installation of thermal insulation on attic ceilings is preferred over windows replacement due to its slightly larger impact on EP_H and EP_{CO2}, along with significantly lower implementation costs. As a result, factor C is consistently set at level +1 in the

top-ranked solutions, while factor B is predominantly at a low level (-1).

The installation of a central heating system and fuel replacement has the largest effect on EP_{CO2} and the second-largest effect on EP_H. However, its implementation cost is reasonably lower than that of thermal insulation on external walls. Although it might be expected that this measure would be preferred at a high level, it is not the case. This is because the weight assigned to EP_H is twice as important as the weight assigned to EP_{CO2}. Consequently, the installation of thermal insulation on external walls is preferred over the installation of a central heating system, except in the solution ranked as 4. Furthermore, the weights assigned to EP_H and EP_{CO2} are six and three times greater than the weight assigned to C_t, respectively, indicating that C_t does not significantly influence the measure preference. Therefore, the installation of a central heating system is used to balance objectives satisfaction and is only partially implemented.

Based on EP_H values and recommendations proposed in Official Gazette of Federation of Bosnia and Herzegovina (2019), the top three solutions can be classified as high energy building class with low energy consumption (class A), while the last two solutions belong to class B.

The total investment costs C_t for the top five ranked solutions range from 14643 to 17 189 €, resulting in significantly lower EP_H and EP_{CO2} compared to the baseline. The best ranked solution achieves an 86.5% reduction in EP_H and 96.8% reduction in EP_{CO2}.

Table 6 displays the specific and absolute final energy for heating, CO₂ emissions, and energy cost savings for the top five ranked solutions. The best ranked solution achieves the highest annual energy, CO₂, and energy cost savings. The SPP is calculated using Eq. (14) and the results are presented in Table 6. The values obtained from the country’s energy statistics, as well as energy and fuel prices, serve as the baseline for estimating energy costs. It is estimated that the annual energy cost for the baseline scenario, which does not involve any energy efficiency retrofit, is approximately 1004 €.

As shown, the SPP ranges from 17.7 to 21 years for the top five ranked solutions, with the best ranked solution having SPP of 19.9 years.

Table 6
Cost-effectiveness analysis of the top five solutions.

Rank	Savings					Economic indicator	
	EP_H (kWh/m ² ann.)	EP_{CO_2} (kg/m ² ann.)	$E_{fin,H}$ (kWh/ann.)	m_{CO_2} (kg/ann.)	C_{sav} (Eur/ann.)	SPP (Year)	
Optimal solutions	1	240.5	20.0	15 729.0	1310.6	862.8	19.9
	2	234.2	17.5	15 315.4	1145.4	845.2	17.7
	3	232.5	19.0	15 206.4	1239.9	832.9	20.4
	4	221.1	19.6	14 458.9	1283.9	790.1	21.0
	5	220.0	16.4	14 389.6	1074.1	794.1	18.4

4. Conclusion

This study specifically focuses on the building type that exhibits the highest energy consumption among all building categories in the country. Consequently, the insights gained from this study hold significant value for integration into national building renovation strategies. The objective of this study is to establish a functional relationship between specific final energy for heating, specific CO₂ emissions, and various building design parameters for a specific residential building type within the country. This is achieved through the use of Full Factorial Design (FFD), which allows for the development of a linear model to predict the specific final energy and CO₂ emissions based on the building's design characteristics. To validate the accuracy of the model, the results were compared with those obtained from a national study on average household energy consumption (Agic et al., 2016).

The findings of this study confirm earlier research, which suggests that upgrading external walls and improving the efficiency of the heating system are the most effective measures for reducing energy consumption and CO₂ emissions. However, it is worth noting that these measures are also the most expensive to implement compared to other retrofit options, resulting in higher overall retrofit costs. In order to minimize specific final energy for heating, specific CO₂ emissions, and retrofit costs, a multi-objective optimization approach is employed for the selected building.

The key points derived from this study can be summarized as follows:

- The FFD methodology enables the establishment of a functional relationship between specific final energy for heating, specific CO₂ emissions, and various building parameters, such as building envelope characteristics, overall system efficiency, and fuel GHG emission factor.
- The analysis of the models indicates that installing thermal insulation on external walls has the greatest impact on reducing specific final energy for heating and specific CO₂ emissions, followed by improving the efficiency of the heating system and utilizing fuels with lower GHG emission factors.
- The cost of an energy efficiency retrofit encompasses material and equipment prices, labor costs, and general expenses, which can be categorized into fixed and variable components. Fixed costs constitute the largest portion of the overall costs, while variable costs fluctuate depending on the level of retrofitting.
- To achieve multi-objective optimization, the NSGA-III genetic algorithm is employed to identify the Pareto front of non-dominated solutions. These solutions represent a set of energy efficiency retrofit measures that yield the lowest specific final energy for heating, specific CO₂ emissions, and overall retrofit costs.
- From the set of non-dominated solutions, the top five ranked solutions with the highest composite desirability functions are analyzed in detail. These solutions include all considered energy efficiency (EE) retrofit measures: installing thermal

insulation on external walls and unheated attic ceiling, replacing windows, and implementing a central heating system along with reducing the fuel GHG emission factor. Implementing high levels of thermal insulation on external walls and attic ceilings is always included, while the implementation levels of the other two measures vary in top five ranked solutions. The best-ranked set of energy efficiency retrofit measures achieves a Simple Payback Period (SPP) of 19.9 years.

CRedit authorship contribution statement

Džana Kadrić: Conceptualization, Methodology, Visualization, Investigation, Writing – original draft, Validation. **Amar Aganović:** Conceptualization, Methodology, Writing – review & editing. **Edin Kadrić:** Conceptualization, Methodology, Investigation, Formal analysis, Data curation, Software.

Declaration of competing interest

The authors declare that they have no known competing financial interests or personal relationships that could have appeared to influence the work reported in this paper.

Data availability

Data will be made available on request

References

- Agic, D., Rizvic, V., Agic, S., 2016. Report of Energy Poverty in Bosnia and Herzegovina.
- Almeida, M., Ferreira, M., 2017. Cost effective energy and carbon emissions optimization in building renovation (Annex 56). Energy Build. 152, 718–738. <http://dx.doi.org/10.1016/j.enbuild.2017.07.050>.
- Arnautović-Aksić, D., et al., 2016. Typology of residential buildings in Bosnia and Herzegovina.
- Ascione, F., Bianco, N., De Stasio, C., Mauro, G.M., Vanoli, G.P., 2017. CASA, cost-optimal analysis by multi-objective optimisation and artificial neural networks: A new framework for the robust assessment of cost-optimal energy retrofit, feasible for any building. Energy Build. 146, 200–219. <http://dx.doi.org/10.1016/j.enbuild.2017.04.069>.
- Ascione, F., Bianco, N., Mauro, G.M., Napolitano, D.F., 2019. Building envelope design: multi-objective optimization to minimize energy consumption, global cost and thermal discomfort. Application to different Italian climatic zones. Energy 174, 359–374.
- Baghoolizadeh, M., Rostamzadeh-Renani, R., Rostamzadeh-Renani, M., Toghraie, D., 2021. A multi-objective optimization of a building's total heating and cooling loads and total costs in various climatic situations using response surface methodology. Energy Rep. 7, 7520–7538. <http://dx.doi.org/10.1016/j.egyr.2021.10.092>.
- Bosnia and Herzegovina Agency for Statistic, 2022a. Annual Report. <https://bhas.gov.ba/>.
- Bosnia and Herzegovina Agency for Statistic, 2022b. Country statistic. <https://bhas.gov.ba/Calendar/Category/26>.
- Bucar, G., 2003. Normativi i Cijene u Graditeljstvu. Sveučilište u Rijeci.
- Carvalho, R.L., Jensen, O.M., Tarelho, L.A.C., 2016. Mapping the performance of wood-burning stoves by installations worldwide. Energy Build. 127, 658–679. <http://dx.doi.org/10.1016/j.enbuild.2016.06.010>.

- Chantrelle, F.P., Lahmidi, H., Keilholz, W., El Mankibi, M., Michel, P., 2011. Development of a multicriteria tool for optimizing the renovation of buildings. *Appl. Energy* 88 (4), 1386–1394. <http://dx.doi.org/10.1016/j.apenergy.2010.10.002>.
- Ciro, G.C., Dugardin, F., Yalaoui, F., Kelly, R., 2016. A NSGA-II and NSGA-III comparison for solving an open shop scheduling problem with resource constraints. *IFAC-PapersOnLine* 49 (12), 1272–1277.
- Costa-Carrapiço, I., Raslan, R., González, J., 2020. A systematic review of genetic algorithm-based multi-objective optimisation for building retrofitting strategies towards energy efficiency. *Energy Build.* 210, 109690. <http://dx.doi.org/10.1016/j.enbuild.2019.109690>.
- Deb, K., Jain, H., 2013. An evolutionary many-objective optimization algorithm using reference-point-based nondominated sorting approach, part I: solving problems with box constraints. *IEEE Trans. Evol. Comput.* 18 (4), 577–601.
- Delgarm, N., Sajadi, B., Delgarm, S., Kowsary, F., 2016a. A novel approach for the simulation-based optimization of the buildings energy consumption using NSGA-II: Case study in Iran. *Energy Build.* 127, 552–560. <http://dx.doi.org/10.1016/j.enbuild.2016.05.052>.
- Delgarm, N., Sajadi, B., Kowsary, F., Delgarm, S., 2016b. Multi-objective optimization of the building energy performance: A simulation-based approach by means of particle swarm optimization (PSO). *Appl. Energy* 170, 293–303. <http://dx.doi.org/10.1016/j.apenergy.2016.02.141>.
- Derringer, G., Suich, R., 1980. Simultaneous optimization of several response variables. *J. Qual. Technol.* 12 (4), 214–219. <http://dx.doi.org/10.1080/00224065.1980.11980968>.
- Došak, J., 2023. Determinants of energy efficient retrofits in residential sector: A comprehensive analysis. *Energy Build.* 282, 112801. <http://dx.doi.org/10.1016/j.enbuild.2023.112801>.
- Emmerich, M.T., Deutz, A.H., 2018. A tutorial on multiobjective optimization: fundamentals and evolutionary methods. *Nat. Comput.* 17 (3), 585–609.
2022. The Energy Community legal framework. [Online]. Available: <https://www.energy-community.org/legal/acquis.html>.
- Energy Community, 2020. National energy and climate plan. [Online]. Available: <https://www.energy-community.org/regionalinitiatives/NECP.html>.
- European Commission, 2020. Communication (2020) 662 - A Renovation Wave for Europe - greening our buildings, creating jobs, improving lives. *Off. J. Eur. Union* 63, [Online]. Available: <https://eur-lex.europa.eu/legal-content/EN/TXT/PDF/?uri=CELEX:52020DC0662&from=EN>.
- European committee for standardization, 2019. EN 16798-1. Comité Européen de Normalisation (CEN).
- European Parliament and Council of the European Union, 2010. Directive 2010/31/EU of the European Parliament and of the Council of 19 May 2010 on the energy performance of buildings. [Online]. Available: <https://eur-lex.europa.eu/legal-content/EN/TXT/?uri=celex%3A32010L0031>.
- European Parliament and Council of the European Union, 2018. Regulation (EU) 2018/1999 on the governance of the Energy Union and climate action. *OJ L* 2018 (1), 1–77, 328, [Online]. Available: <https://eur-lex.europa.eu/legal-content/EN/TXT/PDF/?uri=CELEX:32018R1999&from=EN>.
- European Parliament and Council of the European Union, 2021. Commission delegated regulation (EU) No 244/2012. [Online]. Available: <https://eur-lex.europa.eu/legal-content/EN/TXT/PDF/?uri=CELEX:02010L0031-20210101>.
- Evins, R., 2013. A review of computational optimisation methods applied to sustainable building design. *Renew. Sustain. Energy Rev.* 22, 230–245. <http://dx.doi.org/10.1016/j.rser.2013.02.004>.
- Fan, Y., Xia, X., 2017. A multi-objective optimization model for energy-efficiency building envelope retrofitting plan with rooftop PV system installation and maintenance. *Appl. Energy* 189, 327–335. <http://dx.doi.org/10.1016/j.apenergy.2016.12.077>.
- Ferrara, M., Rolfo, A., Prunotto, F., Fabrizio, E., 2019. EDeSSOpt – Energy Demand and Supply Simultaneous Optimization for cost-optimized design: Application to a multi-family building. *Appl. Energy* 236, 1231–1248. <http://dx.doi.org/10.1016/j.apenergy.2018.12.043>.
- Gao, B., Zhu, X., Ren, J., Ran, J., Kim, M.K., Liu, J., 2023. Multi-objective optimization of energy-saving measures and operation parameters for a newly retrofitted building in future climate conditions: a case study of an office building in Chengdu. *Energy Rep.* 9, 2269–2285. <http://dx.doi.org/10.1016/j.egyr.2023.01.049>.
- García-Cuadrado, J., Conserva, A., Aranda, J., Zambrana-Vasquez, D., García-Armingol, T., Millán, G., 2022. Response surface method to calculate energy savings associated with thermal comfort improvement in buildings. *Sustain.* 14 (5), <http://dx.doi.org/10.3390/su14052933>.
- Hamdy, M., Hasan, A., Siren, K., 2011. Applying a multi-objective optimization approach for design of low-emission cost-effective dwellings. *Build. Environ.* 46 (1), 109–123. <http://dx.doi.org/10.1016/j.buildenv.2010.07.006>.
- Harrington, E.C., 1965. The desirability function. *Ind. Qual. Control* 21 (10), 494–498.
- Hashempour, N., Taherkhani, R., Mahdikhani, M., 2020. Energy performance optimization of existing buildings: A literature review. *Sustain. Cities Soc.* 54, 101967. <http://dx.doi.org/10.1016/j.scs.2019.101967>.
- Ishibuchi, H., Imada, R., Setoguchi, Y., Nojima, Y., 2016. Performance comparison of NSGA-II and NSGA-III on various many-objective test problems. In: 2016 IEEE Congress on Evolutionary Computation (CEC). IEEE, pp. 3045–3052.
- Jafari, A., Valentin, V., 2018a. Proposing a conceptual decision support system for building energy retrofits considering sustainable triple bottom line criteria. In: Construction Research Congress 2018: Sustainable Design and Construction and Education - Selected Papers from the Construction Research Congress 2018, Vol. 2018-April. pp. 553–563. <http://dx.doi.org/10.1061/978078481301.055>.
- Jafari, A., Valentin, V., 2018b. Selection of optimization objectives for decision-making in building energy retrofits. *Build. Environ.* 130, 94–103. <http://dx.doi.org/10.1016/j.buildenv.2017.12.027>.
- Jovanović-Popović, M., et al., 2013. Nacionalna Tipologija Stambenih Zgrada Srbije (National Typology of Residential Buildings in Serbia), no. January. *Fac. Archit. Univ. Belgrade, GIZ - Dtsch. Gesellschaft für Int. Zusammenarbeit*.
- Kadrić, D., Aganovic, A., Kadrić, E., Delalić-Gurda, B., Jackson, S., 2022a. Applying the response surface methodology to predict the energy retrofit performance of the TABULA residential building stock. *J. Build. Eng.* 61 (September), <http://dx.doi.org/10.1016/j.jobe.2022.105307>.
- Kadrić, D., Aganovic, A., Martinović, S., Delalić, N., Delalić-Gurda, B., 2022b. Cost-related analysis of implementing energy-efficient retrofit measures in the residential building sector of a middle-income country – A case study of Bosnia and Herzegovina. *Energy Build.* 257, 111765. <http://dx.doi.org/10.1016/j.enbuild.2021.111765>.
- Kolokotsa, D., Diakaki, C., Grigoroudis, E., Stavrakakis, G., Kalaitzakis, K., 2009. Decision support methodologies on the energy efficiency and energy management in buildings. *Adv. Build. Energy Res.* 3 (1), <http://dx.doi.org/10.3763/aber.2009.0305>.
- Liu, B., Pouramini, S., 2021. Multi-objective optimization for thermal comfort enhancement and greenhouse gas emission reduction in residential buildings applying retrofitting measures by an Enhanced Water Strider Optimization Algorithm: A case study. *Energy Rep.* 7, 1915–1929, 6, p. 109945, Jun. 2020, <http://dx.doi.org/10.1016/j.enbuild.2020.109945>.
- Lu, Y., Wang, S., Zhao, Y., Yan, C., 2015. Renewable energy system optimization of low/zero energy buildings using single-objective and multi-objective optimization methods. *Energy Build.* 89, 61–75. <http://dx.doi.org/10.1016/j.enbuild.2014.12.032>.
- Mauro, G.M., Hamdy, M., Vanoli, G.P., Bianco, N., Hensen, J.L.M., 2015. A new methodology for investigating the cost-optimality of energy retrofitting a building category. *Energy Build.* 107, 456–478. <http://dx.doi.org/10.1016/j.enbuild.2015.08.044>.
- MOFTER, 2021. 5th Annual Report under the Energy Efficiency Directive. European Parliament, [Online]. Available: <https://www.energy-community.org/documents/parties/EE.html>.
- Mostafazadeh, F., Eirdmousa, S.J., Tavakolan, M., 2023. Energy, economic and comfort optimization of building retrofits considering climate change: A simulation-based NSGA-III approach. *Energy Build.* 280, 112721. <http://dx.doi.org/10.1016/j.enbuild.2022.112721>.
- Neufert, E., Neufert, P., 2012. Neufert Architects' Data, fourth ed. *Journal of Chemical Information and Modeling*.
- Nydahl, H., Andersson, S., Åstrand, A.P., Olofsson, T., 2019. Including future climate induced cost when assessing building refurbishment performance. *Energy Build.* 203, 0–5. <http://dx.doi.org/10.1016/j.enbuild.2019.109428>.
- N. 40/6. Official Gazette of Bosnia and Herzegovina, Bosnia and Herzegovina National Energy Efficiency Action Plan (NEEAP) 2016–2018, 2017..
- N. 81/19. Official Gazette of Federation of Bosnia and Herzegovina, 2019. Rulebook on Minimum Requirements for Energy Performance of Buildings. [Online]. Available: <http://www.ee-infos.ba/Content/docs/pravilnikominimalnimzahjtevima.pdf>.
- Pajek, L., Jevrić, M., Čipranić, I., Košir, M., 2023. A multi-aspect approach to energy retrofitting under global warming: A case of a multi-apartment building in Montenegro. *J. Build. Eng.* 63 (September 2022), 105462. <http://dx.doi.org/10.1016/j.jobe.2022.105462>.
- Pinzon Amoroch, J.A., Hartmann, T., 2022. A multi-criteria decision-making framework for residential building renovation using pairwise comparison and TOPSIS methods. *J. Build. Eng.* 53 (May), 104596. <http://dx.doi.org/10.1016/j.jobe.2022.104596>.
- Publications Office of the European Union, 2019. European Union. EU Energy in Figures. Statistical Pocketbook 2019. Luxembourg, <http://dx.doi.org/10.2833/197947>.
- Roberti, F., Oberegger, U.F., Lucchi, E., Troi, A., 2017. Energy retrofit and conservation of a historic building using multi-objective optimization and an analytic hierarchy process. *Energy Build.* 138, 1–10. <http://dx.doi.org/10.1016/j.enbuild.2016.12.028>.

- Rosso, F., Ciancio, V., Dell'Olmo, J., Salata, F., 2017. Multi-objective optimization of building retrofit in the Mediterranean climate by means of genetic algorithm application. *Energy Build.* 21.
- Ruggeri, A.G., Gabrielli, L., Scarpa, M., 2020. Energy retrofit in european building portfolios: A review of five key aspects. *Sustain.* 12 (18), 1–37. <http://dx.doi.org/10.3390/SU12187465>.
- Sadeghifam, A.N., Zahraee, S.M., Meynagh, M.M., Kiani, I., 2015. Combined use of design of experiment and dynamic building simulation in assessment of energy efficiency in tropical residential buildings. *Energy Build.* 86, 525–533. <http://dx.doi.org/10.1016/j.enbuild.2014.10.052>.
- Shao, Y., G, P., Lang, W., 2014. Integrating requirement analysis and multi-objective optimization for office building energy retrofit strategies. *Energy Build.* 82, 356–368. <http://dx.doi.org/10.1016/j.enbuild.2014.07.030>.
- Sharif, S.A., Hammad, A., 2017. Simulation-based multi-objective optimization of institutional building renovation considering energy consumption, life-cycle cost and life-cycle assessment. *J. Build. Eng.* 21, 429–445.
- Sharif, S.A., Hammad, A., 2019. Simulation-Based Multi-Objective Optimization of institutional building renovation considering energy consumption, Life-Cycle Cost and Life-Cycle Assessment. *J. Build. Eng.* 21, 429–445. <http://dx.doi.org/10.1016/j.jobe.2018.11.006>.
- Shen, P., Braham, W., Yi, Y., Eaton, E., 2019. Rapid multi-objective optimization with multi-year future weather condition and decision-making support for building retrofit. *Energy* 172, 892–912. <http://dx.doi.org/10.1016/j.energy.2019.01.164>.
- Tootkaboni, M.P., Ballarini, I., Corrado, V., 2021. Analysing the future energy performance of residential buildings in the most populated Italian climatic zone: A study of climate change impacts. *Energy Rep.* 7, 8548–8560. <http://dx.doi.org/10.1016/j.egy.2021.04.012>.
- Tuominen, P., Klobut, K., Tolman, A., Adjei, A., De Best-Waldhober, M., 2012. Energy savings potential in buildings and overcoming market barriers in member states of the European Union. *Energy Build.* 51, 48–55. <http://dx.doi.org/10.1016/j.enbuild.2012.04.015>.
- US Department of Energy, 2022. Energy plus. [Online]. Available: <https://www.energy.gov/eere/buildings/downloads/energyplus-0>.
- Wang, N., 2023. Multi-objective energy saving optimization of residential buildings based on MABC-BP. *Energy Rep.* (ISSN: 2352-4847) 9 (Supplement 7), 922–929. <http://dx.doi.org/10.1016/j.egy.2023.04.182>.
- Wang, C., Kilkis, S., Tjernström, J., Nyblom, J., Martinac, I., 2017. Multi-objective optimization and parametric analysis of energy system designs for the Albano University Campus in Stockholm. *Procedia Eng.* 180 (December), 621–630. <http://dx.doi.org/10.1016/j.proeng.2017.04.221>.
- Yong, Z., Li-juan, Y., Qian, Z., Xiao-yan, S., 2020. Multi-objective optimization of building energy performance using a particle swarm optimizer with less control parameters. *J. Build. Eng.* 32, 101505. <http://dx.doi.org/10.1016/j.jobe.2020.101505>.
- Zhang, H., Hewage, K., Prabatha, T., Sadiq, R., 2021. Life cycle thinking-based energy retrofits evaluation framework for Canadian residences: A Pareto optimization approach. *Build. Environ.* 204, 108115. <http://dx.doi.org/10.1016/j.BUILDENV.2021.108115>.